J|A|C|S
ARTICLES
Published on Web 08/28/2004

Catalytic Probe Lithography: Catalyst-Functionalized Scanning Probes as Nanopens for Nanofabrication on Self-Assembled Monolayers

Mária Péter, Xue-Mei Li, Jurriaan Huskens,* and David N. Reinhoudt*

Contribution from the Laboratory of Supramolecular Chemistry and Technology, MESA+ Institute for Nanotechnology, University of Twente, P.O. Box 217, 7500 AE Enschede, The Netherlands

Received April 6, 2004; E-mail: j.huskens@utwente.nl; d.n.reinhoudt@utwente.nl

Abstract: This article describes the use of scanning catalytic probe lithography for nanofabrication of patterns on self-assembled monolayers (SAMs) of reactive adsorbates. Catalytic writing was carried out by scanning over bis(*ω*-*tert*-butyldimethyl-siloxyundecyl)disulfide SAMs using 2-mercapto-5-benzimidazole sulfonic acid-functionalized gold-coated AFM tips. The acidic tips induced local hydrolysis of the silyl ether moieties in the contacted areas, and thus patterned surfaces were created. Diffusion effects arising from the use of an ink were excluded in these type of experiments, and therefore structures with well-defined shapes and sizes were produced. The smallest lines drawn by this technique were about 25 nm wide, corresponding to the actual contact area of the tip. Lateral force microscopy studies performed on different SAMs helped to clarify the nature and cause of the friction contrasts observed by AFM. Dendritic wedges with thiol functions inserted into the catalytically written areas, thus enhancing the height contrast. The created patterns open possibilities to build 3D nanostructures.

Introduction

Nanometer control over the positioning and size of various surface-confined chemical functionalities would enable one to design sensing materials with large capacities and to detect single molecules.[1−4] Top-down and bottom-up manufacturing approaches or combinations of those are the key technologies used to fabricate nanostructures.[5]

Optical lithography is one of the most commonly used lithographic techniques in the top-down approach.[6] However, it becomes extremely expensive and difficult when features below 100 nm have to be produced.[7] Moreover, this technique can be used with a limited number of substrates and does not offer control over the chemistry of patterned surfaces. There are new nano- and microfabrication technologies, such as microcontact printing (μCP)[8] and dip-pen nanolithography (DPN),[9] both using self-assembly as the key feature to produce patterned surfaces. Self-organization of thiols or disulfides, for example, onto gold leads to the formation of self-assembled monolayers (SAMs), the fabrication and properties of which have been described extensively.[10−13]

μCP is a soft lithography technique, which uses a patterned elastomer, such as poly(dimethylsiloxane) (PDMS), as a stamp.[5,8,14−16] SAMs are formed only in the contacted areas. The smallest reported feature produced by μCP is about 50 nm.[15,17,18]

Scanning probe lithography (SPL) is based on the use of a scanning probe to create nanopatterns under environmental conditions.[19−25] Patterns are created mechanically (by scratching) or by using electrical current.[24,25] SPL techniques are serial and, therefore in general slow, but this drawback might be overcome by the introduction of probe arrays.[35,36] The main SPL techniques using SAMs utilize elimination, addition, and substitution lithographies. DPN is an addition lithography tech-

(1) Drexler, K. E. *Engines of Creation, The Coming Era of Nanotechnology*; Anchor Books Doubleday: New York, 1986.
(2) Ozin, G. A. *Adv. Mater.* **1992**, *4*, 612−649.
(3) Malsch, I. *Nanotechnology* **1999**, *10*, 1−7.
(4) Collins, P. G.; Zettl, A.; Bando, H.; Thess, A.; Smalley, R. E. *Science* **1997**, *278*, 100−103.
(5) Xia, Y.; Whitesides, G. M. *Angew. Chem., Int. Ed.* **1998**, *37*, 550−575.
(6) Campbell, S. A. *The Science and Engineering of Microelectronic Fabrication*; Oxford University Press: Oxford, 1996.
(7) Tennant, D. M. *Limits of Conventional Lithography*; Timp, G., Ed.; Springer: New York, 1999.
(8) Kumar, A.; Whitesides, G. M. *Appl. Phys. Lett.* **1993**, *63*, 2002−2004.
(9) Piner, R. D.; Zhu, J.; Xu, F.; Hong, S. F.; Mirkin, C. A. *Science* **1999**, *283*, 661−663.
(10) Ulman, A. *An Introduction to Ultrathin Organic Films from Langmuir-Blodgett To Self-Assembly*; Academic Press: New York, 1991.
(11) Schreiber, F. *Prog. Surf. Sci.* **2000**, *65*, 151−256.
(12) Dubois, L. H.; Nuzzo, R. G. *Annu. Rev. Phys. Chem.* **1992**, *43*, 437−463.
(13) Poirier, G. E. *Chem. Rev.* **1997**, *97*, 1117−1127.
(14) Xia, Y.; Rogers, J. A.; Paul, K. E.; Whitesides, G. M. *Chem. Rev.* **1999**, *99*, 1823−1848.
(15) Odom, T. W.; Thalladi, V. R.; Love, J. C.; Whitesides, G. M. *J. Am. Chem. Soc.* **2002**, *124*, 12112−12113.
(16) Xia, Y.; Whitesides, G. M. *Annu. Rev. Mater. Sci.* **1998**, *28*, 153−184.
(17) Li, H.-W.; Muir, B. V. O.; Fichet, G.; Huck, W. T. S. *Langmuir* **2003**, *19*, 1963−1965.
(18) Michel, B.; Bernard, A.; Bietsch, A.; Delamarche, E.; Geissler, M.; Juncker, D.; Kind, H.; Renault, J.-P.; Rothuizen, H.; Schmid, H.; Schmidt-Winkel, P.; Stutz, R.; Wolf, H. *IBM J. Res. Dev.* **2001**, *45*, 697−719.
(19) Cavallini, M. *Science* **2003**, *299*, 662.
(20) Cavallini, M.; Biscarini, F.; Leon, S.; Zerbetto, F.; Bottari, G.; Leigh, D. A. *Science* **2003**, *299*, 531.
(21) Eigler, D. M.; Schweizer, E. K. *Nature* **1990**, *344*, 524−526.
(22) McCarty, G. S.; Weiss, P. S. *Chem. Rev.* **1999**, *99*, 1983−1990.
(23) Nyffenegger, R. M.; Penner, R. M. *Chem. Rev.* **1997**, *97*, 1195−1230.
(24) Krämer, S.; Fuierer, R. R.; Gorman, C. B. *Chem. Rev.* **2003**, *103*, 4367−4418.
(25) Maoz, R.; Cohen, S. R.; Sagiv, J. *Adv. Mater.* **1999**, *11*, 55−61.

10.1021/ja048027w CCC: $27.50

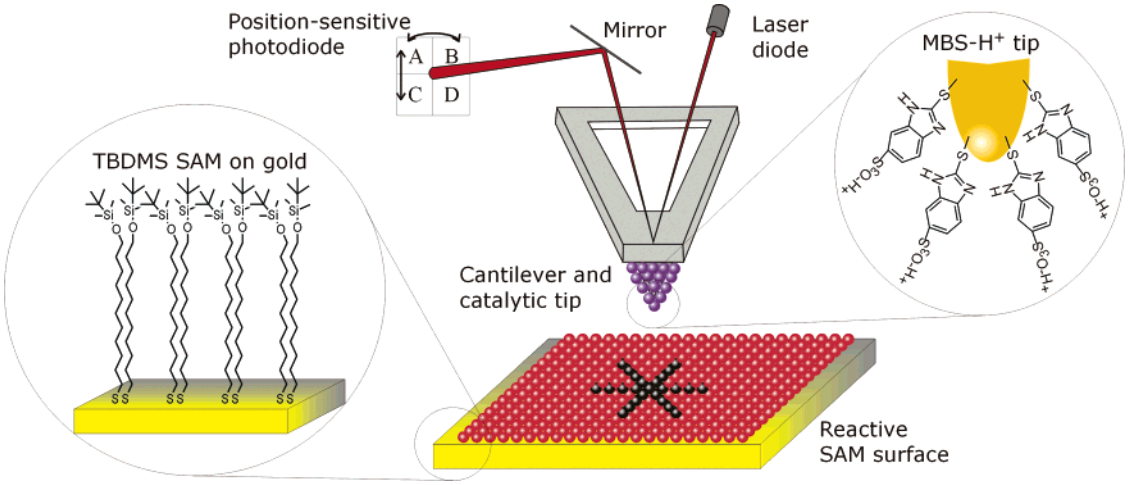

Figure 1. Schematic illustration of scanning catalytic probe lithography performed on a TBDMS SAM on gold using a gold-coated AFM tip covered with MBS−H^+.

nique providing an elegant way to write chemical nanopatterns on various surfaces in specific areas.[9,26−30] It uses a scanning probe coated with the desired material to be transferred to the substrate. By scanning the surface, the ink will be transported from the tip to the substrate through the presence of a water meniscus. The mechanism of ink transport in DPN is not fully understood, the amount of ink transferred is not controllable, and the ink diffusion determines the pattern sizes created depending on temperature, humidity, ink nature, and contact time.[31−34] These disadvantages may be overcome when scanning probe lithography is performed without the use of an ink.

There are only a few articles that describe the use of a catalytically active atomic force microscopy (AFM) tip.[37−41] In an early first attempt, Schultz et al. showed that by using Pt-coated AFM tips, the terminal azide groups of a monolayer on glass could be locally reduced to amino groups.[37] To our knowledge, the use of a catalyst-functionalized AFM tip for lithographic applications was never reported before.

We have previously reported the printing of sulfonic acid-functionalized gold nanoparticles for pattern creation on reactive SAMs.[42] In this approach, the reactivity of the immobilized catalyst was tested for the hydrolysis of a reactive trimethylsilyl (TMS) ether SAM, serving as a model system for a study of the surface−surface reactivity and tip−surface catalysis. A gold-coated, acid-functionalized AFM tip can be envisaged to behave in a way similar to the acid-functionalized gold colloids when brought into contact with a silyl ether SAM. We show in this article that 2-mercapto-5-benzoimidazole sulfonic acid (MBS−H^+)-functionalized AFM tips can be used to locally induce a surface hydrolysis reaction and thus create patterns on the nanometer level.

Results and Discussion

The preparation of the bis(*ω*-*tert*-butyldimethyl-siloxyundecyl)disulfide (TBDMS) adsorbate has been described elsewhere.[43] Self-assembled monolayers of the TBDMS adsorbate, 11-mercapto-1-undecanol (MUD), and 1-octadecanethiol (ODT) were prepared by dipping freshly cleaned gold substrates into 1.0 mM adsorbate solutions in dichloromethane for 3 h. The substrates were taken out, rinsed thoroughly with dichloromethane, ethanol, and water, and dried in a stream of N_2. Functionalized AFM tips were prepared by dipping gold-coated tips into a 1.0 mM solution of sodium 5-mercapto-2-benzimidazole sulfonate (MBS−Na^+) in methanol for 14 h. The tips were taken out, rinsed with methanol and water, and dried. The activation of the functionalized tips was performed by dipping them into a 0.1 M aqueous HCl solution for a few minutes followed by rinsing with water and drying.

Catalytic Probe Lithography on TBDMS SAMs. Functionalized AFM tips were employed for the catalytic pattern creation in TBDMS SAMs. The experiments were carried out in air. The principles of the experiment are illustrated in Figure 1. The TBDMS layer was scanned in the desired areas with an AFM tip functionalized with MBS−H^+. The resulting patterns were read using the same pen. Initially, a $3 \times 3\ \mu m^2$ area was scanned with a minimized normal load (<10 nN) at a scan angle of 90°. After the area was scanned four times with a scan rate of 1 Hz, a larger surface scan ($6 \times 6\ \mu m^2$) was taken at a scan angle of 45° without withdrawing the tip and using the same scan speed. Height and friction images were recorded simultaneously as shown in Figure 2. The height image (Figure 2a) does not show any features, indicating there is neither mechanical deformation of the SAM nor material removal by scratching. The friction profile (Figure 2b) shows a rhomb in the middle

(26) Hong, S.; Zhu, J.; Mirkin, C. A. *Science* **1999**, *286*, 523−525.
(27) Hong, S.; Zhu, J.; Mirkin, C. A. *Langmuir* **1999**, *15*, 7897−7900.
(28) Ivanisevic, A.; McCumber, K. V.; Mirkin, C. A. *J. Am. Chem. Soc.* **2002**, *124*, 11997−12001.
(29) Zhang, Y.; Salaita, K.; Lim, J. H.; Mirkin, C. A. *Nano Lett.* **2002**, *2*, 1389−1392.
(30) Weinberger, D. A.; Hong, S.; Mirkin, C. A.; Wessels, B. W.; Higgins, T. B. *Adv. Mater.* **2000**, *12*, 1600−1603.
(31) Jang, J.; Hong, S.; Schatz, G. C.; Ratner, M. A. *J. Chem. Phys.* **2001**, *115*, 2721−2729.
(32) Jang, J.; Schatz, G. C.; Ratner, M. A. *J. Chem. Phys.* **2002**, *116*, 3875−3886.
(33) Sheehan, P. E.; Whitman, L. J. *Phys. Rev. Lett.* **2002**, *88*, 156104.
(34) Schwartz, P. V. *Langmuir* **2002**, *18*, 4041−4046.
(35) Hong, S.; Mirkin, C. A. *Science* **2000**, *288*, 1808−1811.
(36) Zhang, M.; Bullen, D.; Chung, S. W.; Hong, S.; Ryu, K. S.; Fan, Z. F.; Mirkin, C. A.; Liu, C. *Nanotechnology* **2002**, *13*, 212−217.
(37) Müller, W. T.; Klein, D. L.; Lee, T.; Clarke, J.; McEuen, P. L.; Schultz, P. G. *Science* **1995**, *268*, 272−273.
(38) Blasdel, L. K.; Banerjee, S.; Wong. S. S. *Langmuir* **2002**, *18*, 5055−5057.
(39) Wang, J.; Kenseth, J. R.; Jones, V. W.; Green, J.-B. D.; McDermott, M. T.; Porter, M. D. *J. Am. Chem. Soc.* **1997**, *119*, 12796−12799.
(40) Blackledge, C.; Egebretson, D. A.; McDonald, J. D. *Langmuir* **2000**, *16*, 8317−8323.
(41) Pavlovic, E.; Oscarsson, S.; Quist, A. P. *Nano Lett.* **2003**, *3*, 779−781.
(42) Li, X.-M.; Paraschiv, V.; Huskens, J.; Reinhoudt, D. N. *J. Am. Chem. Soc.* **2003**, *125*, 4279−4284.
(43) Li, X.-M.; Péter, M.; Huskens, J.; Reinhoudt, D. N. *Nano Lett.* **2003**, *3*, 1449−1453.

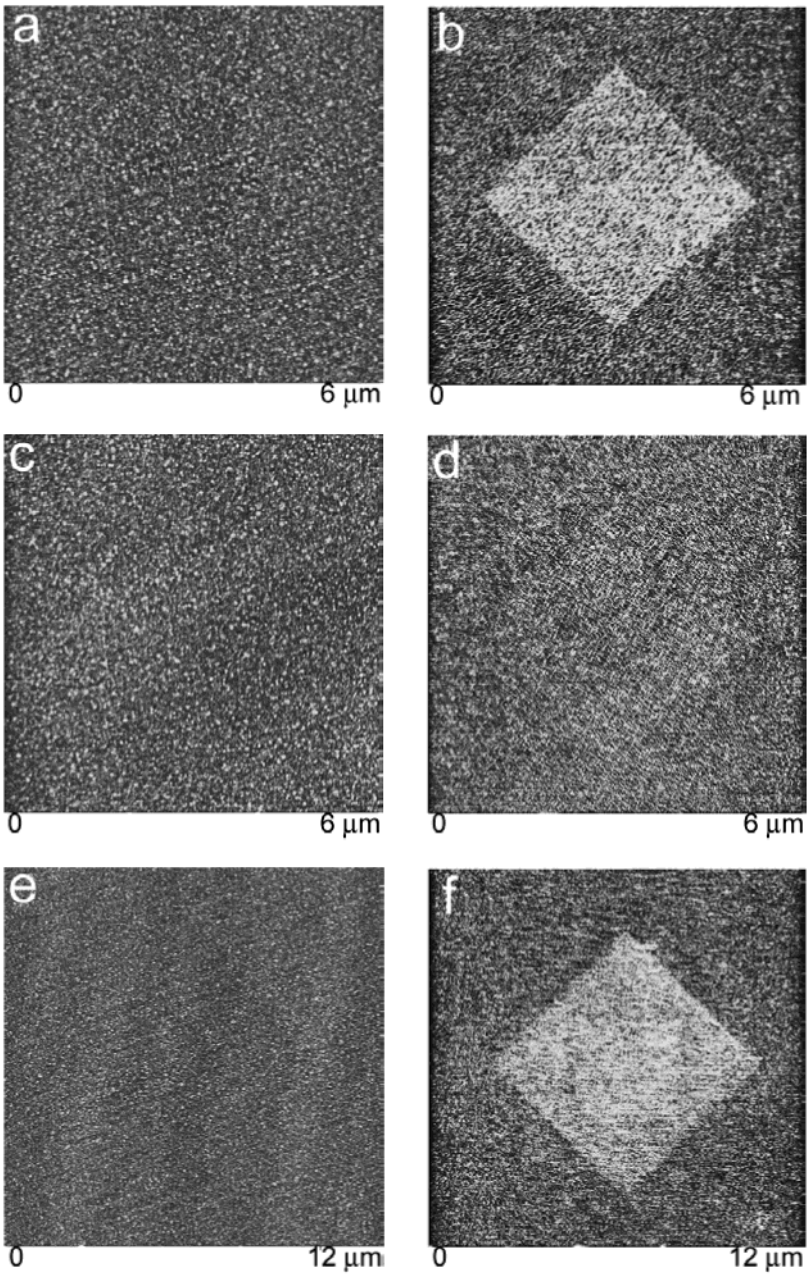

Figure 2. AFM height (a, c, e; z range 5 nm) and friction (b, d, f; z range 0.1 V) images of a TBDMS SAM during continuous catalytic pattern creation with a MBS−H^+-functionalized AFM tip in air. (a, b) Scanning a 3 × 3 μm^2 area four times followed by one scan of a 6 × 6 μm^2 area at 45°. (c, d) The same after continued scanning of the 6 × 6 μm^2 area. (e, f) After zooming out to 12 × 12 μm^2 and scanning at 90°.

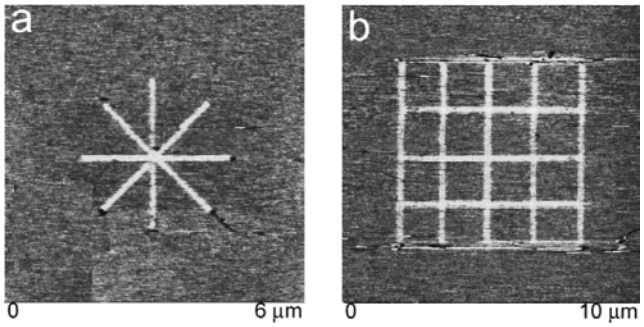

Figure 3. AFM friction images (z range 0.2 V) of nanostructures created on TBDMS SAMs by catalytic probe lithography. (a) Scan size 6 × 6 μm^2. (b) 10 × 10 μm^2.

that is brighter than the rest of the surface. This rhomb with higher friction corresponds to the initially scanned area (3 × 3 μm^2), and the friction contrast is attributed to the cleavage of TBDMS moieties. After scanning four times, the contrast in the image diminished (Figures 2c, height and 2d, friction). This loss of contrast indicates a continuous reaction of the surface groups as a result of the scanning. After changing the scan angle back to 90° and increasing the scanned area to 12 × 12 μm^2, a new rhomb appeared in the center of the image (Figure 2f, friction). The height image still did not show any features (Figure 2e). The borders of the initially scanned 3 × 3 μm^2 area were still faintly visible within the newly created rhomb (Figure 2f). The patterning process was reproduced at least three times using different activated tips and different TBDMS SAM samples.

Structures with well-defined shapes and sizes were created using CPL in TBDMS SAMs (Figure 3). The aspect ratio of

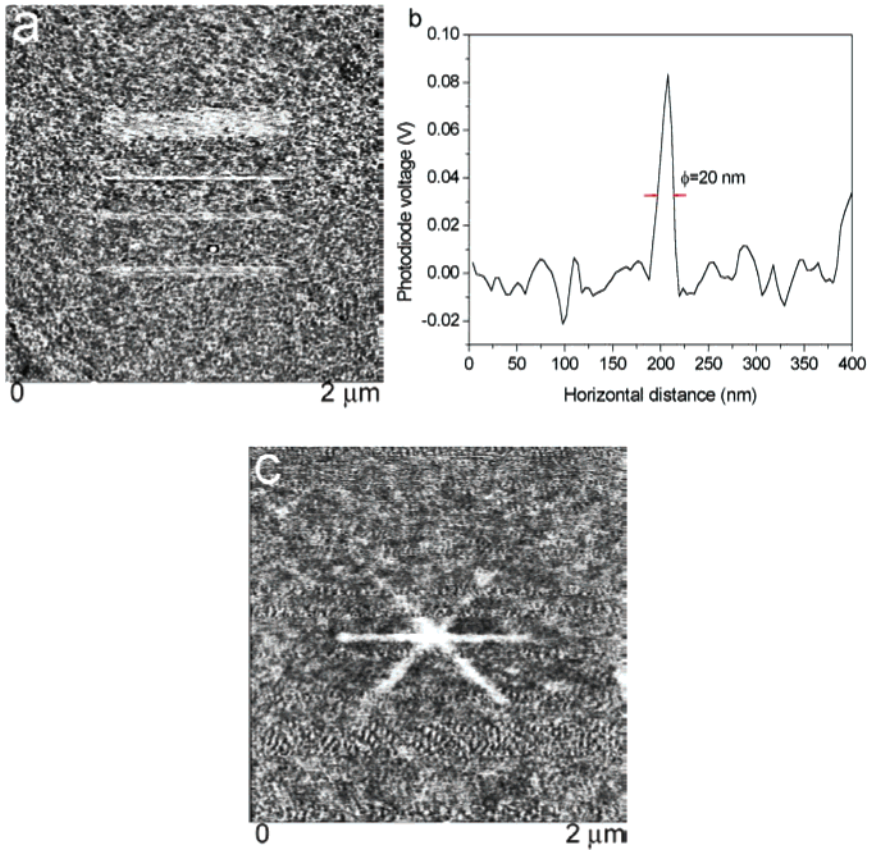

Figure 4. (a, c) AFM friction images (z range 0.2 V) of nanostructures created on TBDMS SAMs by catalytic probe lithography (z range 0.1 V; scan size 2×2 μm^2). (b) Line trace through the second line from the top in Figure 4a.

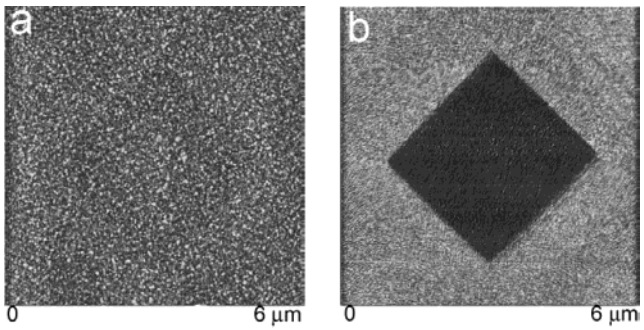

Figure 5. AFM height (a; z range 5 nm) and friction (b; z range 0.2 V) images (scan size 6×6 μm^2) of a TBDMS SAM after scanning with an inactive functionalized tip and zoomed out at a scan angle of 45°.

the images, the *x* and *y* scan offset, and the scan angles were adjusted in such a way as to achieve the desired structures. For easy visualization, line widths of about 100 nm were drawn. The smallest line produced was about 25 nm (Figure 4a,b). Since the use of an ink is excluded in these experiments, the resolution of the structures is limited only by the actual contact area between the AFM tip and the substrate and possible drifts in the piezoelectric scanner.

Control Experiments Performed with Catalytically Inactive Tips on TBDMS and ODT SAMs in Air. Two types of catalytically inactive tips were used, tips functionalized with $MBS-Na^+$ but not protonated and bare Si_3N_4 tips. Figure 5 shows AFM pictures recorded after enlarging an area on a TBDMS SAM, which was initially scanned with a nonactivated tip. In the height image, no significant features are observed. However, a dark rhomb (lower friction) appeared in the friction image. Continuous pattern creation was observed even while scanning with these nonactivated tips (images not shown). The use of bare Si_3N_4 tips also produced patterns with lower friction. The same experiment was carried out on a ODT SAM on gold. For this system, no patterns were observed in the scanned regions. As a result of these observations, we believe that TBDMS SAMs develop a "memory" upon scanning because of their specific nature and structure. The packing density of the chains in these SAMs is lower as compared to that of an alkanethiol SAM with the same chain length because of the relatively large end groups. Therefore, the tip may induce reorientation and reorganization of the surface groups during scanning, giving rise to areas of lower friction. Annealing the surface should restore the system to thermodynamic equilibrium, thus removing any changes caused by tip-induced orientation.

Liu and Bhushan have reported tip-induced reorientation in biphenyl thiol SAMs.[44] The SAMs were scanned in a certain area with an AFM tip gradually increasing the normal load applied. After enlarging the scan area and decreasing the load, the previously scanned area showed lower friction. This phenomenon was attributed to the compression and orientation of the SAM under the applied load.

Because of the bulky surface groups, the TBDMS adsorbates produce poorly ordered SAMs with low packing densities. The molecules might be reoriented during the sliding of the tip over the surface, producing a better packing of the tail groups, which in turn is expected to result in an area of lower friction. To verify whether this assumption is correct and to clarify the

(44) Liu, H.; Bhushan, B. *Ultramicroscopy* **2002**, *91*, 177−183.

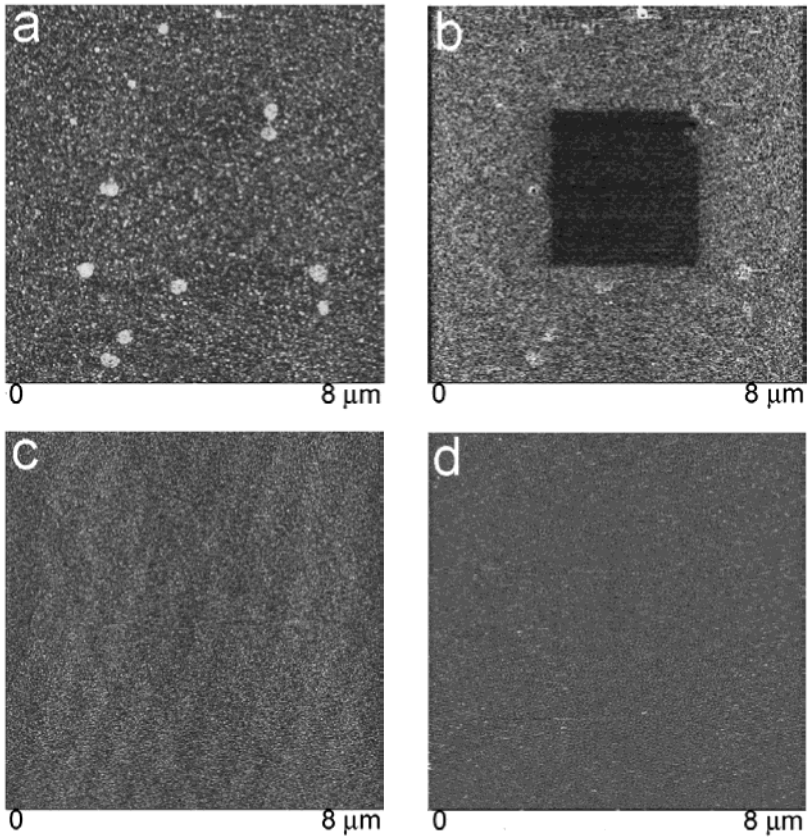

Figure 6. AFM height (a, c; z range 5 nm) and friction (b, d; z range 0.1 V) images of TBDMS (a, b) and ODT SAMs (c, d) after the friction study was performed with a Si_3N_4 tip on an $3 \times 3\ \mu m^2$ area using lateral force microscopy and zooming out to $8 \times 8\ \mu m^2$.

friction contrasts that can be expected for the different layers as a function of the applied load, qualitative friction studies were performed.

Friction Studies Performed on TBDMS and Control SAMs. We have shown above that scanning TBDMS SAMs with a catalytically active tip resulted in areas of higher friction while inactive tips created areas of lower friction. To clarify these differences in friction contrast, we carried out friction studies using lateral force microscopy. A series of SAMs on gold were prepared: TBDMS, MUD, ODT, and hydrolyzed TBDMS layers. The hydrolyzed TBDMS SAM was prepared by dipping a TBDMS layer into a solution of monolayer-protected gold nanoparticles functionalized with $MBS-H^+$ for 30 min.[42]

Pyramidal Si_3N_4 tips with a nominal spring constant of 0.32 Nm^{-1} were used. Within one series of layers, the experiments were performed using the same tip, without any readjustment of the incoming laser beam position on the cantilever. The relative humidity of the air was 20.5%. The scanned area was $3 \times 3\ \mu m^2$. The scan angle was set to 90°. The scan speed was set to 1 Hz. The normal load was changed at the end of each image by adjusting the setpoint value. The applied load was gradually increased from 1 to 33 nN as determined by analyzing the force−distance curves. The "friction force" was determined by taking half the difference between the left-to-right and right-to-left lateral deflection forces, i.e., the half-width of the friction loop. The reported values are in volts. As this study targeted a qualitative comparison between the friction properties of the different SAMs, no quantitative evaluation of friction forces has been attempted since this would require the determination of the torsional spring constant of the cantilever.

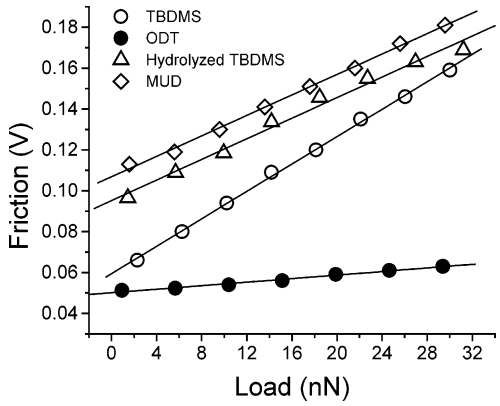

Figure 7. Friction of different SAMs plotted versus load.

After the friction study was completed, a larger area was scanned as is shown in Figure 6. For the TBDMS SAMs, no significant difference was observed in the height image (Figure 6a), indicating no physical damage or material removal. Darker areas appeared in the middle of the friction image (Figure 6b), indicating tip-induced reorientation.[44] A similar behavior was found for the hydrolyzed TBDMS SAMs (not shown). Friction experiments performed on ODT SAMs did not result in any changes in the height or friction images (Figure 6c,d). An ODT SAM is well-packed and therefore is expected to behave like a spring. Monte Carlo simulations of ODT SAMs showed that after the release of compression the original conformation is restored almost immediately.[44] Scanning MUD SAMs resulted in material accumulation at the borders of the image, indicating some material removal. This can easily be explained if one considers that in the case of MUD SAMs bilayers can be formed.

Scheme 1. Dendritic Wedge Insertion into Hydrolyzed TBDMS SAMs

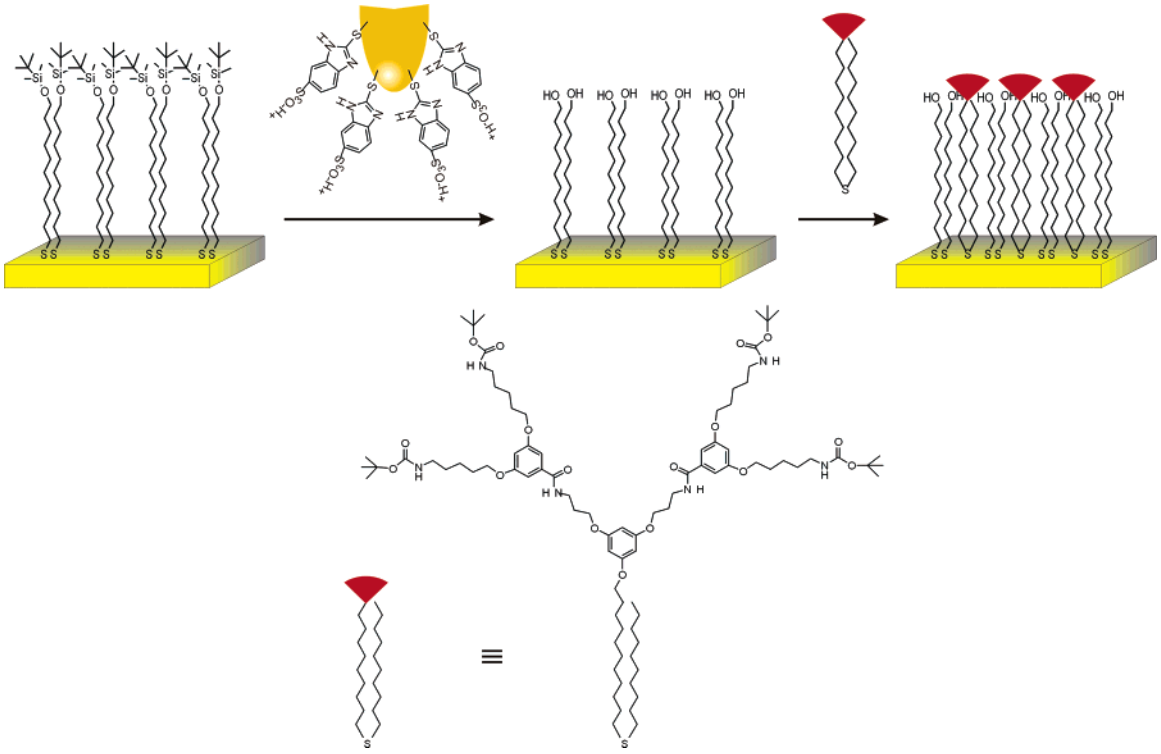

The friction (in volts) was plotted as a function of the applied load (Figure 7). The friction changes linearly with the load for all layers. The individual friction coefficients for each layer can be determined from the slope of the curves.[45,46] Unlike macroscopic materials, the friction at small scale depends on the adhesion as well, which leads to nonzero friction even without load.[45,46] In the applied load range, the friction for these SAMs followed the order: ODT < TBDMS < hydrolyzed TBDMS < MUD. ODT SAMs showed the lowest friction. This is in good agreement with tribology studies performed on methyl-terminated SAMs that can be used as effective molecular lubricants.[47,48] TBDMS SAMs showed significantly higher friction as compared to ODT SAMs, which is attributed to the less well-ordered surface groups. Hydrolyzed TBDMS SAMs presented even higher friction than TBDMS SAMs. According to Figure 7, the hydrolyzed TBDMS SAMs have the same friction coefficient (slope) as the MUD SAMs, as can be expected because both present hydroxyl groups to the surface. However, under the same load, an MUD SAM shows a higher friction due to better order. The friction study showed that for the applied load range a contrast reversal was not expected for the different layers. This indicates that one always expects to observe a higher friction for the hydrolyzed TBDMS SAMs than for the non-hydrolyzed layers if operated below a certain load.

Chemical Functionalization of the Created Patterns. Chemical amplification of the created patterns is an important step toward further applications. The advancing contact angle with water of a TBDMS SAM is 84°, indicating a hydrophobic layer. The huge difference between the advancing and receding ($\theta_r = 25°$) contact angles indicates a poor order of the layers because of the presence of the bulky terminal groups. The bulky groups are removed from the surface after hydrolysis, leaving unfilled spaces between the remaining alkyl chains. These "defects" can be filled with different types of ligands, such as a dendritic wedge, as is shown in Scheme 1. The dendritic wedge can serve as a promising building block for nanofabrication because of its highly branched structure that allows easy functionalization of the core and/or the periphery. It has been shown in our laboratory that dendritic adsorbates can be inserted into preformed SAMs via a dialkylsulfide chain, making use of the fact that surface-bound thiols can be replaced by thiols or sulfides from solution.[49,50] The mechanism of surface-confinement relies on the formation of defects in the alkanethiol monolayer.[51] Isolated dendrimers with an average height of 3.3 nm in a decanethiol monolayer could be converted into larger dendritic structures by metal−ligand coordination, achieving a height of 7.5 nm.[50]

The samples, after CPL of a square of 10 × 10 μm^2, were dipped into a dendritic wedge solution in dichloromethane for 1.5 h. The samples were removed from the solution, rinsed with dichloromethane, dried, and imaged with AFM. Figure 8 shows that the height image presents a clear difference in height that corresponds to about 1.3 nm. The height change is observed only in the area on which the catalytic pattern creation was performed. This proves that indeed cleavage of the TBDMS moieties took place in the areas scanned with a catalytically

(45) Noy, A.; Frisbie, C. D.; Rozsnyai, L. F.; Wrighton, M. S.; Lieber, C. M. *J. Am. Chem. Soc.* **1995**, *117*, 7943−7951.
(46) van der Vegte, E. W.; Hadziioannou, G. *Langmuir* **1997**, *13*, 4357−4368.
(47) Liu, H.; Bhushan, B. *Ultramicroscopy* **2002**, *91*, 185−202.
(48) Bhushan, B. *Wear* **2001**, *250*, 1105−1123.
(49) Friggeri, A.; van Manen, H.-J.; Auletta, T.; Li, X.-M.; Zapotoczny, S.; Schönherr, H.; Vancso, G. J.; Huskens, J.; van Veggel, F. C. J. M.; Reinhoudt, D. N. *J. Am. Chem. Soc.* **2001**, *123*, 6388−6395.
(50) van Manen, H.-J.; Auletta, T.; Dordi, B.; Schönherr, H.; Vancso, G. J.; van Veggel, F. C. J. M.; Reinhoudt, D. N. *Adv. Funct. Mater.* **2002**, *12*, 811−818.
(51) Friggeri, A.; Schönherr, H.; van Manen, H.-J.; Huisman, B.-H.; Vancso, G. J.; Huskens, J.; van Veggel, F. C. J. M.; Reinhoudt, D. N. *Langmuir* **2000**, *16*, 7757−7763.

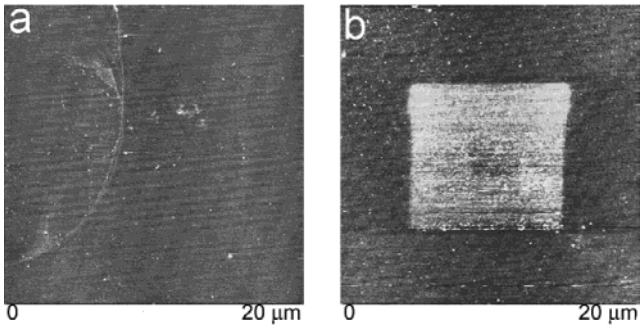

Figure 8. AFM height images (z range 5 nm) showing TBDMS SAMs after CPL before (a; scan size 20 × 20 μm^2) and after (b; scan size 20 × 20 μm^2) chemical pattern enhancement by insertion of a dendritic wedge.

active AFM tip. Test experiments were performed on samples scanned with nonactivated or bare Si_3N_4 tips, which were also dipped into the solution of the dendritic wedge. For these samples no adsorption of the dendritic wedge was observed.

Experimental Section

Chemicals. All chemicals were used as received, unless otherwise stated. MUD and ODT were purchased from Aldrich. Water was purified by Millipore membrane unit. Solvents used for monolayer preparation were of reagent grade. The preparation of the TBDMS adsorbate has been described elsewhere.[43] The preparation of MBS−H^+-functionalized gold nanoparticles and their application as ink for lithographic pattern creation have been described elsewhere.[42] The synthesis of the dendritic wedge has been described elsewhere.[50]

Monolayer Preparation. All glassware used for monolayer preparation was cleaned in piranha solution (concentrated H_2SO_4 and 30% aqueous H_2O_2 in a ratio of 3:1). *Warning:* Piranha solution should be handled with great caution, because it has been reported to detonate unexpectedly. The glassware was rinsed with large amounts of water (Millipore). Gold-coated SiO_x wafers were supplied by Ssens BV (The Netherlands) (2−5 nm of Ti followed by the evaporation of 20 nm of gold). The gold substrates were cleaned with O_2 plasma prior to use. SAMs were prepared by immersing the gold substrates into 1.0 mM solution of the corresponding adsorbates at room temperature for 3 h. The SAMs were rinsed with dichloromethane, ethanol, and water and dried in a stream of N_2.

Nanofabrication with Functionalized AFM Tips. Gold-coated AFM tips were prepared by Ssens BV (The Netherlands) by the evaporation of 2 nm of Ti followed by 50 nm of gold onto Si_3N_4 AFM probes (Veeco Instruments). The tips were rinsed with copious amounts of dichloromethane, dried, and then placed into a 1.0 mM solution of MBS−Na^+ in methanol overnight. The tips were taken out, rinsed with methanol and water, and dried. Before use, the tips were activated by dipping them into a 0.1 M aqueous HCl solution for a few minutes and then rinsed thoroughly with water and methanol. Pattern creation on TBDMS SAMs using functionalized AFM tips was carried out with a commercial AFM system (Nanoscope III, Veeco, Digital Instruments). The writing process was performed in air at a scan rate of 1 Hz (1 line/s). The normal load applied to the surface was always kept below 10 nN to avoid physical damage of the SAMs. A higher load range was applied just during the friction study.

Friction Study. Si_3N_4 AFM tips with a nominal spring constant of 0.32 $N \cdot m^{-1}$ were used. Within one series of samples, the same tip was used throughout the experiments. The scanned area was 3 × 3 μm^2. The scan angle was set to 90°. The normal load was changed at the end of each image by adjusting the setpoint value. The applied load was increased from 1.0 to 33.0 nN. The friction force was determined by taking half the difference between the left-to-right and right-to-left lateral deflection forces, i.e., the half width of the friction loop. The reported values are in volts.

Conclusions

This article describes the use of chemically functionalized AFM tips to fabricate patterns in TBDMS SAMs by scanning catalytic probe lithography. MBS−H^+-functionalized tips were employed as catalysts to induce local hydrolysis on the scanned areas. The smallest structure drawn was about 25 nm, which is comparable to the contact area between tip and substrate. Difficulties encountered due to diffusion effects are excluded utilizing this technique because there is no ink transfer involved in the pattern creation.

Friction studies indicated that in the applied load range hydrolyzed areas presented higher friction while a lower friction corresponded to tip-induced reorientation of the large tail groups. The successful chemical amplification of written patterns using a dendritic wedge solution proved that indeed hydrolysis took place in the scanned areas, leading to a less dense SAM structure and allowing the insertion of the dendritic wedge. The dendritic wedge allows further functionalization into, for example, multifunctional nanoscale sensors.

The cleavage process is truly catalytic as deduced from the following reasoning. When it is assumed (i) that the density of MBS−H^+ groups on the tip is approximately the same as the density of TBDMS groups at the SAMs and (ii) that all TBDMS groups are hydrolyzed, the turnover number is simply the ratio between the written area and the contact area between tip and substrate. Thus, turnover numbers can be estimated to be as large as 6×10^4 (for a 6 × 6 μm^2 area, Figure 2e,f, written with a contact area of 25 × 25 nm^2).

Our study clearly shows that this type of scanning probe technique may form a versatile component toward the realization of a true nanomanufacturing paradigm.

Acknowledgment. This research was supported by the Technology Foundation STW, applied science division of NWO, and the technology program of the Ministry of Economic Affairs (Simon Stevin Nanolithography Award to D.N.R., Project No. TST-4946). Henk-Jan van Manen is acknowledged for the synthesis of the dendritic wedge.

JA048027W